Dalton Transactions

Accepted Manuscript

ROYAL SOCIETY OF CHEMISTRY

www.rsc.org/dalton

Journal Name

RSCPublishing

ARTICLE

Long-lived and Oxygen-Responsive Photoluminescence in the Solid State of Copper(I) Complexes Bearing Fluorinated Diphosphine and Bipyridine Ligands

Cite this: DOI: 10.1039/x0xx00000x

Received 00th January 2012,
Accepted 00th January 2012

DOI: 10.1039/x0xx00000x

www.rsc.org/

Michihiro Nishikawa, Yuri Wakita, Tatsuya Nishi, Takumi Miura, Taro Tsubomura*

Luminescence properties of a family of newly synthesized copper(I) complexes bearing 2,2′-bipyridine derivative and 1,2-bis(dipentafluorophenyl)phosphinoethane (dfppe), [Cu(diimine)(dfppe)]PF_6, were investigated. The quantum yield and the lifetime of the emission of [Cu(6dmbpy)(dfppe)]PF_6 (6dmbpy = 6,6′-dimethyl-2,2′-bipyridine) in the solid state under argon (Φ = 9%, τ = 16, 180 μs), which is one of the longest lifetimes among all copper(I) complexes bearing diimine and diphosphine, are much larger than those under air (Φ < 0.5%, τ = 1.5, 8.0 μs). Crystal packing, structural rearrangement in the excited state, and nature of the transitions are important for the photophysics of dfppe complexes. The voids in the crystals as well as the very long lifetime of the excited states play a key role for oxygen responsive photoluminescence in the solid state.

Introduction

Long-lived photoexcited states of metal complexes such as polypyridyl ruthenium(II) complexes[1] attract much attention for light-emitting devices,[2,3] molecular machines,[4,5] and photocatalysts.[6] Optical oxygen sensors, which are often based on quenching of long-lived photoluminescence of the metal complexes in solutions, sol-gels, and polymer films, are important for biology, medicine, and environmental analysis.[7-9] The number of reports for the oxygen-responsive emission in the solid state is very limited because oxygen is basically difficult to diffuse inside of the crystals to quench the photoluminescence. Recently, the oxygen responsive photoluminescence in the solid state based on ruthenium(II) and copper(I) complexes have been attracting much attention for their high sensitivities, stabilities, and fast responses.[10-13] The lifetimes of the emission of these crystals, which have oxygen-accessible voids, are very long, therefore, the luminescence is quenched by oxygen molecule even in the solid state.[10-13]

Copper(I) complexes bearing diimine and diphosphine are one of the promising candidates for photofunctional materials.[11-34] Many copper(I) complexes are known to exhibit thermally activated delayed fluorescence at room temperature, because the difference in the energy levels between the singlet and triplet excited states of the complexes is small.[29] The absorption and luminescence in the visible light region based on charge transfer (CT) from the atomic orbitals made of both copper and phosphine to π* orbitals of diimine moieties are often observed in the complexes.[14-18] The bulky substituents positioned toward metal centre, such as the introduction of the methyl groups on 2- and 9-position of 1,10-phenanthroline in copper(I) complexes, have been known to increase the quantum yield, the lifetime, and the energy of the emission due to following reasons: (i) inhibiting the structural rearrangement in the excited states, because the structural distortion typically leads to a red shift in emission which reduces the energy gap; this cause the reduction of the lifetime and the quantum yields of the emission through the enhancement of the non-radiative constant, (ii) preventing the coordination of the solvent to the copper centre which leads to the deactivation of the excited state via non-emissive species, and the access of solvent is assisted by the structural distortion mentioned in (i).[14-18] The

Scheme 1. Synthesis of copper(I) complexes.

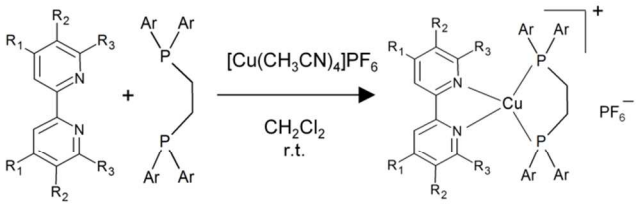

		Ar	R_1	R_2	R_3
1·PF_6	[Cu(bpy)(dppe)]PF_6	C_6H_5	H	H	H
2·PF_6	[Cu(4dmbpy)(dppe)]PF_6	C_6H_5	Me	H	H
3·PF_6	[Cu(bpy)(dfppe)]PF_6	C_6F_5	H	H	H
4·PF_6	[Cu(4dmbpy)(dfppe)]PF_6	C_6F_5	Me	H	H
5·PF_6	[Cu(6dmbpy)(dfppe)]PF_6	C_6F_5	H	H	Me
6·PF_6	[Cu(MeObpy)(dfppe)]PF_6	C_6F_5	MeO	H	H
7·PF_6	[Cu(5dmbpy)(dfppe)]PF_6:	C_6F_5	H	Me	H

substitution effects on the luminescence of the copper(I) complexes have been also observed in the solid state.[30]

We have developed several highly emissive copper(I) complexes bearing diimine and diphosphine.[31-34] Metal complexes bearing 1,2-bis[bis(pentafluorophenyl)phosphine]ethane (dfppe) such as rhodium(III)[35] and platinum(II)[36] complexes have been reported. To the best of our knowledge, this is the first report of the copper(I) complexes bearing dfppe ligands. Since the pentafluorophenyl group is generally one of the strongest electron withdrawing groups,[35,36] the luminescence behaviors of dfppe complexes are expected to be drastically changed from those of dppe complexes. Here, we investigate the photophysics of a family of the copper(I) complexes of $[Cu(bpy)(dppe)]PF_6$ (**1**·PF_6, bpy = 2,2′-bipyridine, dppe = 1,2-bis(diphenylphosphino)ethane)[26] and newly synthesized six complexes, $[Cu(4dmbpy)(dppe)]PF_6$ (**2**·PF_6, 4dmbpy = 4,4′-dimethyl-2,2′-bipyridine), $[Cu(bpy)(dfppe)]PF_6$ (**3**·PF_6), $[Cu(4dmbpy)(dfppe)]PF_6$ (**4**·PF_6), $[Cu(6dmbpy)(dfppe)]PF_6$ (**5**·PF_6, 6dmbpy = 6,6′-dimethyl-2,2′-bipyridine), $[Cu(MeObpy)(dfppe)]PF_6$ (**6**·PF_6, MeObpy = 4,4′-dimethoxy-2,2′-bipyridine), and $[Cu(5dmbpy)(dfppe)]PF_6$ (**7**·PF_6, 5dmbpy = 5,5′-dimethyl-2,2′-bipyridine) (Scheme 1). In these complexes, **5**·PF_6 shows very long lifetime of the excited state (16 and 180 μs dual exponential) and interesting oxygen responsive photoluminescence in the solid state.

Experimental

Materials and Methods

Reagents and solvents were purchased from commercial suppliers and used without further purification. Tetrakis(acetonitrile)copper(I) hexafluorophosphate ($[Cu(MeCN)_4]PF_6$) was synthesized according to the methods described in the literature.[37] ^{1}H-NMR and ^{19}F-NMR spectra in acetone-d_6 were recorded on a JEOL Delta-500 spectrometer using tetramethylsilane (δ = 0.00 ppm, ^{1}H) as an internal standard,[38a] and neat monofluorobenzene (δ = –113.1 ppm, ^{19}F)[38b] as an external standard. Emission spectra in the solution state were obtained in a solvent degassed by 10 min. argon bubbling. Since the absorption around 450 nm due to bis(diimine) complex gradually appears in CH_2Cl_2 solution of $\mathbf{5}^+$, the measurements were performed immediately after dissolving the compounds in a solvent degassed by at least five freeze-pump-thaw cycles using a quartz cell fitted with a Teflon vacuum stop cock. The solid samples, which are obtained from CH_2Cl_2-diethylether solution, well grounded, and dried in vacuum, are employed for photophysical measurements. Infrared (IR) spectra were measured on a JASCO FT/IR-460 plus spectrometer using KBr pellets. Absorption spectra were measured on a Shimadzu UV-3100 spectrometer or an Agilent 8453 spectrometer. Emission spectra and emission lifetimes were collected on a laboratory-made apparatus. For the steady state emission spectra, a degassed sample solution was excited by a monochromated Xe lamp (a 75 W lamp connected to an Oriel Cornerstone 130 monochromator) and the emission was collected through a quartz fiber and fed into a spectrometer equipped with a cooled CCD sensor (Ocean Optics model QE65000). Emission quantum yields in the solution state were obtained using quinine bisulfate (1.0×10^{-5} M) in 1N H_2SO_4 as a standard (Φ = 0.60).[39] For the measurement of emission decay, the sample was excited by a N_2 laser (Usho, KEN-1520), and the emission was focused on a 20 cm monochromator (Jovin Yvon H-20). The emission light was detected by a photomultiplier tube, Hamamatsu R928, and the signal was digitized by an oscilloscope (Tektronix TDS5034). Absolute quantum yields of the luminescence in the solid state were determined with the apparatus equipped with a Labsphere integrating sphere (4P-GPS-033-SL). The quantum yields were measured by using the samples which were spread all over a quartz petri dish (i. d. = 1.3 cm) or a screw-capped 1 mm optical-path quartz cell with rubber septum. Samples for photophysical measurements under argon and the oxygen were obtained by argon flow and the oxygen flow, respectively in the 1 mm cell. Samples for photophysical measurements in vacuum were obtained by using a 1 mm length quartz cell fitted with a Teflon vacuum stop cock. Time course of the emission intensities was measured on a JASCO FP-6500 spectrometer.

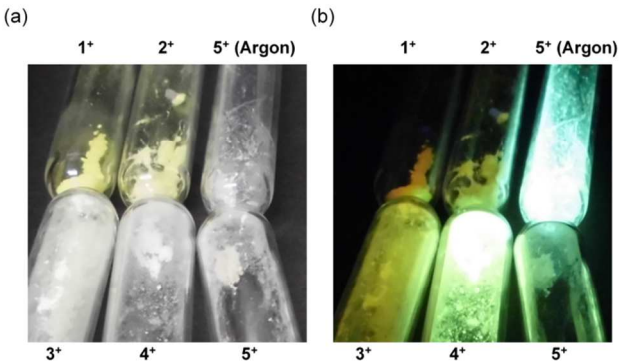

Fig. 1. The photos of the complexes at room temperature under room light (a) and under UV light (b). The samples are placed in air and argon.

Synthesis

$[Cu(bpy)(dppe)]BF_4$ (1·PF_6). **1**·PF_6[26] was prepared according to similar methods to procedures of **2·PF_6** described in the next paragraph.

$[Cu(4dmbpy)(dppe)]BF_4$ (2·PF_6). Under an argon atmosphere, $[Cu(MeCN)_4]PF_6$ (74 mg, 0.199 mmol) was added to dppe (80 mg, 0.201 mmol) in a 5 mL dichloromethane. Then, 4dmbpy (36 mg, 0.195 mmol) was added. The reaction mixture was stirred for 30 min. at room temperature. Diethyl ether was added to the solution to precipitate the product as a solid, which was filtered, washed with diethyl ether, and dried in vacuo: yield, 138 mg (0.174 mmol, 89%). ^{1}H NMR (500 MHz, acetone-d_6): δ 8.63 (s, 2H), 8.52 (d, J = 5 Hz, 2H), 7.5-7.4 (m, 22H), 3.53 (t, J = 8 Hz, 4H), 2.62 (s, 6H). ^{19}F NMR (471 MHz, acetone-d_6): δ –72.5 (d, J = 710 Hz, PF_6^-). Elemental analysis. Calculated for $C_{38}H_{36}N_2P_3F_6Cu$: C, 57.69; H, 4.59; N, 3.54. Found C, 57.19; H, 4.39; N, 3.56. Other heteroleptic complexes were prepared in a similar manner described above.

$[Cu(bpy)(dfppe)]PF_6$ (3·PF_6). $[Cu(MeCN)_4]PF_6$ (37 mg, 0.099 mmol), dfppe (76 mg, 0.100 mmol), and bpy (15 mg, 0.096 mmol): yield, 68 mg (0.061 mmol, 63%). ^{1}H NMR (500 MHz, acetone-d_6): δ 8.80 (d, J = 8 Hz, 2H), 8.62 (d, J = 5 Hz, 2H), 8.37 (td, J = 8, 2 Hz, 2H), 7.74 (ddd, J = 8, 5, 2 Hz, 2H), 3.56 (t, J = 9 Hz, 4H). ^{19}F NMR (471 MHz, acetone-d_6): δ –72.6 (d, J = 710 Hz, PF_6^-), –131.0 (m, C_6F_5), –149.2 (m, C_6F_5), –161.4 (m, C_6F_5). Elemental analysis. Calculated for $CuC_{36}H_{12}N_2P_3F_{26}$: C 38.51, H 1.08, N 2.49. Found C 38.15, H 1.27, N 2.41.

$[Cu(4dmbpy)(dfppe)]PF_6$ (4·PF_6). $[Cu(MeCN)_4]PF_6$ (37 mg, 0.099 mmol), dfppe (76 mg, 0.100 mmol), and 4dmbpy (18 mg, 0.098 mmol): yield, 76 mg (0.066 mmol, 68%). ^{1}H NMR

(500 MHz, acetone-d_6): δ 8.63 (s, 2H), 8.42 (d, J = 5 Hz, 2H), 7.54 (d, J = 5 Hz, 2H), 3.53 (t, J = 8 Hz, 4H), 2.62 (s, 6H). ^{19}F NMR (471 MHz, acetone-d_6): δ –72.7 (d, J = 710 Hz, PF_6^-), –130.9 (m, C_6F_5), –149.3 (m, C_6F_5), –161.5 (m, C_6F_5). Calculated for $CuC_{38}H_{16}N_2P_3F_{26}$: C 39.65, H 1.40, N 2.43. Found C 39.70, H 1.51, N 2.43.

[Cu(6dmbpy)(dfppe)]PF$_6$ (5·PF$_6$). [Cu(MeCN)$_4$]PF$_6$ (39 mg, 0.105 mmol), dfppe (76 mg, 0.100 mmol), and 6dmbpy (19 mg, 0.103 mmol): yield, 90 mg (0.078 mmol, 78%). ^{1}H NMR (500 MHz, acetone-d_6): δ 8.60 (d, J = 8 Hz, 2H), 8.26 (t, J = 8 Hz, 2H), 7.66 (d, J = 8 Hz, 2H), 3.77 (t, J = 9 Hz, 4H), 2.27 (s, 6H). ^{19}F NMR (471 MHz, acetone-d_6): δ –72.6 (d, J = 710 Hz, PF_6^-), –131.2 (m, C_6F_5), –148.7 (m, C_6F_5), –161.0 (m, C_6F_5). Calculated for $C_{38}H_{16}N_2P_3F_{26}Cu$: C, 39.65; H, 1.40; N, 2.43. Found C, 39.55; H, 1.19; N, 2.38.

[Cu(MeObpy)(dfppe)]PF$_6$ (6·PF$_6$). [Cu(MeCN)$_4$]PF$_6$ (19 mg, 0.051 mmol), dfppe (38 mg, 0.050 mmol), and MeObpy (10 mg, 0.046 mmol): yield, 21 mg (0.018 mmol, 38%). ^{1}H NMR (500 MHz, acetone-d_6): δ 8.37 (d, J = 6 Hz, 2H), 8.29 (d, J = 2 Hz, 2H), 7.24 (dd, J = 6, 2 Hz, 2H), 4.13 (s, 6H), 3.51 (t, J = 9 Hz, 4H). ^{19}F NMR (471 MHz, acetone-d_6): δ –72.6 (d, J = 710 Hz, PF_6^-), –131.0 (m, C_6F_5), –149.4 (m, C_6F_5), –161.5 (m, C_6F_5). Calculated for $C_{38}H_{16}N_2P_3O_2F_{26}Cu$: C, 38.58; H, 1.36; N, 2.37. Found C, 37.90; H, 1.43; N, 2.74.

[Cu(5dmbpy)(dfppe)]PF$_6$ (7·PF$_6$). [Cu(MeCN)$_4$]PF$_6$ (19 mg, 0.050 mmol), dfppe (38 mg, 0.050 mmol), and 5dmbpy (9 mg, 0.049 mmol): yield, 48 mg (0.042 mmol, 84%). ^{1}H NMR (500 MHz, acetone-d_6): δ 8.61 (d, J = 8 Hz, 2H), 8.41 (s, 2H), 8.16 (d, J = 8 Hz, 2H), 3.54 (t, J = 8 Hz, 4H), 2.36 (s, 6H). ^{19}F NMR (471 MHz, acetone-d_6): δ –72.8 (d, J = 708 Hz, PF_6^-), –131.0 (m, C_6F_5), –149.7 (m, C_6F_5), –161.6 (m, C_6F_5). Calculated for $C_{38}H_{16}N_2P_3F_{26}Cu$: C, 39.65; H, 1.40; N, 2.43. Found C, 39.25; H, 1.30; N, 2.54.

X-ray Structural Analysis. X-ray crystallographic measurements of **2**·PF$_6$, **4**·PF$_6$·(CH$_3$)$_2$CO, **5**·PF$_6$, **6**·PF$_6$·(CH$_3$)$_2$CO, and **7**·PF$_6$ were made on a Rigaku Saturn 70 CCD area detector with graphite-monochromated MoKα radiation. Images were collected and the data were processed by using the *CrystalClear*.[40a] The structures were solved by direct methods *SIR-92*[40b] and refined by the full matrix least squares procedures (*SHELXL-97*).[40c] All calculations were performed by using the *CrystalStructure*[40d] or *Wingx*[40e] crystallographic software package. Crystallographic data have been deposited with Cambridge Crystallographic Data Centre: Deposition number CCDC-1042034 for **2**·PF$_6$, CCDC-1042035 for **4**·PF$_6$·(CH$_3$)$_2$CO, CCDC-1042036 for **5**·PF$_6$, CCDC-1042037 for **6**·PF$_6$·(CH$_3$)$_2$CO, and CCDC-1042038 for **7**·PF$_6$·C$_6$H$_{14}$. Copies of the data can be obtained free of charge via http://www.ccdc.cam.ac.uk/conts/retrieving.html. Single crystals suitable for analysis were obtained by following procedures: (i) slow diffusion of hexane in acetone solution of **4**·PF$_6$, **6**·PF$_6$, and **7**·PF$_6$, (ii) slow diffusion of diethylether in dichloromethane solution of **5**·PF$_6$, (iii) slow diffusion of hexane in dichloromethane solution of **2**·PF$_6$. The void spaces are calculated from volumes of total potential solvent area per unit cell by using PLATON CALC SOLV option. Disordered crystal solvents of **4**·PF$_6$·(CH$_3$)$_2$CO were removed by SQUEEZE option.[40f]

DFT calculation. Calculation was performed using Gaussian 03W software[41] with the B3LYP[42-44] method using the atomic coordinates determined by X-ray. TDDFT was used to calculate singlet and triplet excited state energies. Basis sets were as follows: copper 6-311G with Wachters's 4p functions,[45] phosphorus and nitrogen 6-31G*+, fluorine, oxygen, and carbon 6-31G*, and hydrogen 6-31G. Population analysis was carried out by *AOMIX* software.[46] The pictures of the orbitals have been depicted with *MOLKEL* software.[47]

Results and discussion

A family of copper(I) complexes was newly synthesized by a reaction of [Cu(CH$_3$CN)$_4$]PF$_6$, diimine, and diphosphine ligands in dichloromethane at room temperature (Scheme 1). The compounds were characterized by ^{1}H NMR, elemental analysis, and single-crystal X-ray structural analysis. The NMR spectra of the complexes bearing dppe, **1**$^+$ and **2**$^+$, are characteristic of the heteroleptic copper(I) complexes. The ^{1}H NMR spectra of the complexes bearing dfppe, **3**$^+$, **4**$^+$, **5**$^+$, **6**$^+$ and **7**$^+$, show one set of signals due to the aromatic groups in the bipyridine moieties and the methylene groups in the diphosphine moieties, suggesting that the heteroleptic complexes are stable in air-saturated solution. The ^{19}F NMR spectra of the dfppe complexes show signals due to the pentafluorophenyl groups as well as the hexafluorophosphate counterion. Attempts to prepare [Cu(6dmbpy)(dppe)]PF$_6$ by using a procedure similar to that described for **2**·PF$_6$ gave red solid of [Cu(6dmbpy)$_2$]PF$_6$.[48,49] We found that the colors of the dfppe complexes, **3**·PF$_6$, **4**·PF$_6$, **5**·PF$_6$, **6**·PF$_6$, and **7**·PF$_6$ in the solid state are much lighter than those of dppe complexes, **1**·PF$_6$ and **2**·PF$_6$ (Fig. 1), and the dfppe complexes exhibit more intense photoluminescence than the dppe complexes under the UV light excitation. Fig. 1 is representative photographs of an oxygen responsive photoluminescence in the solid state of **5**·PF$_6$; the luminescence intensity looks to be weak under air and strong under argon atmosphere.

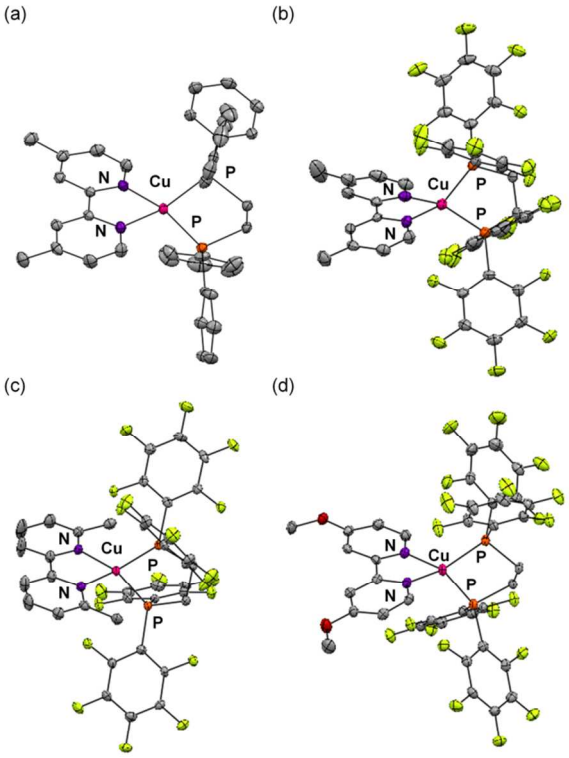

Fig. 2. The crystal structures of the complex cations of **2**$^+$ (a), **4**$^+$ (b), **5**$^+$ (c), and **6**$^+$ (d). Hydrogens, counterions, and solvent molecules are omitted for clarity.

Table 1. Crystal data for $2{\cdot}PF_6$, $4{\cdot}PF_6{\cdot}(CH_3)_2CO$, $5{\cdot}PF_6$, $6{\cdot}PF_6{\cdot}(CH_3)_2CO$, and $7{\cdot}PF_6{\cdot}0.5C_6H_{14}$.

complex	$2{\cdot}PF_6$	$4{\cdot}PF_6{\cdot}(CH_3)_2CO$	$5{\cdot}PF_6$	$6{\cdot}PF_6{\cdot}(CH_3)_2CO$	$7{\cdot}PF_6{\cdot}0.5C_6H_{14}$
empirical formula	$C_{38}H_{36}CuF_6N_2P_3$	$C_{41}H_{22}CuF_{26}N_2OP_3$	$C_{38}H_{16}CuF_{26}N_2P_3$	$C_{41}H_{26}CuF_{26}N_2O_3P_3$	$C_{41}H_{23}CuF_{26}N_2P_3$
formula weight	791.14	1209.06	1150.98	1245.09	1194.06
crystal system	Monoclinic	Orthorhombic	Triclinic	Monoclinic	Monoclinic
temperature / K	123	123	123	123	123
space group	$P2_1/c$ (#14)	$Pcab$(#61)	$P\bar{1}$(#2)	$P2_1/c$ (#14)	$P2_1/c$ (#14)
a / Å	10.573(3)	20.0258 (9)	11.7046 (19)	13.290 (5)	11.5047 (10)
b / Å	18.382(5)	20.3253 (9)	11.9986 (18)	19.920 (6)	33.521 (3)
c / Å	18.979(5)	23.2280 (11)	15.584 (2)	20.107 (5)	23.333 (2)
α / °	90	90	91.946 (7)	90	90
β / °	99.449(1)	93.5035(7)	96.639 (7)	122.495 (16)	98.828 (1)
γ / °	90	90	101.608 (7)	90	90
Vol / Å^3	3638.5(17)	9454.5 (7)	2125.8 (6)	4490 (2)	5761.4(4)
Z	4	8	2	4	8
D_{calcd} / g cm^{-3}	1.444	1.699	1.798	1.842	1.784
μ / mm^{-1}	0.793	0.7	0.78	0.75	0.74
R (I>2σ(I))	0.074	0.078	0.074	0.054	0.083
wR (all)	0.182	0.146	0.211	0.111	0.16
GOF	1.093	1.35	1.08	1.19	1.2
$\Delta\rho_{max}$ / e-Å^{-3}	2.47	0.63	3.33	0.52	1.62
$\Delta\rho_{min}$ / e-Å^{-3}	-0.90	-0.44	-0.69	-0.44	-0.69

Table 2. Crystal data for $2{\cdot}PF_6$, $4{\cdot}PF_6{\cdot}(CH_3)_2CO$, $5{\cdot}PF_6$, $6{\cdot}PF_6{\cdot}(CH_3)_2CO$, and $7{\cdot}PF_6{\cdot}0.5C_6H_{14}$.

complex	$2{\cdot}PF_6$	$4{\cdot}PF_6{\cdot}(CH_3)_2CO$	$5{\cdot}PF_6$	$6{\cdot}PF_6{\cdot}(CH_3)_2CO$	$7{\cdot}PF_6{\cdot}0.5C_6H_{14}$[c]
Cu1—N1	2.022 (3)	2.018 (3)	2.025 (4)	2.023 (2)	2.034 (4), 2.015(3)
Cu1—N2	2.040 (3)	2.026 (3)	2.041 (4)	2.027 (2)	2.039 (4), 2.058(4)
Cu1—P1	2.2328(11)	2.2370 (10)	2.2425(15)	2.2265 (11)	2.2218(12), 2.2400(12)
Cu1—P2	2.2482(11)	2.2505 (11)	2.2659(15)	2.2807 (9)	2.2759(12), 2.2577(12)
N1—Cu1—N2	80.77 (13)	81.47 (12)	82.65 (18)	81.51 (9)	81.77(15), 81.49(14)
P1—Cu1—P2	91.65 (4)	91.14 (4)	92.01 (5)	91.32 (3)	91.04 (4), 91.27(4)
α[a]	86.4	85.9	88.0	85.8	82.3, 78.3
β_1, β_2[b]	2.8	10.8	6.1	11.9	3.73, 19.0

[a] The dihedral angles specified by the two planes, which are determined by the coordinates of the Cu1, N1 and N2 atoms and the Cu1, P1 and P2 atoms, respectively. [b] The dihedral angles between the mean planes of two pyridine moieties in bpy ligand. [c] Two complex cations are observed in asymmetric unit of $7{\cdot}PF_6{\cdot}0.5C_6H_{14}$.

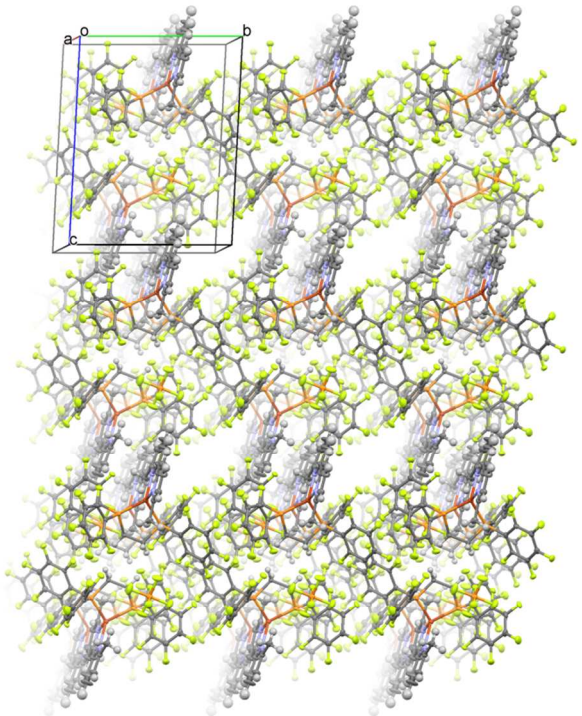

Fig. 3. The crystal structures of $5{\cdot}PF_6$.

Crystallographic parameters, important bond lengths and angles, and ORTEP views of crystal structures of $2{\cdot}PF_6$, $4{\cdot}PF_6{\cdot}(CH_3)_2CO$, $5{\cdot}PF_6$, $6{\cdot}PF_6{\cdot}(CH_3)_2CO$, and $7{\cdot}PF_6{\cdot}0.5C_6H_{14}$ are shown in Tables 1 and 2, Fig. 2, and Supporting Information Figs. S1-S5 and Table S1. The structures of heteroleptic mononuclear copper(I) complexes bearing two bidentate ligands, diimine and diphosphine, with tetrahedral coordination geometry are confirmed in a family of the complexes. The bond lengths, angles, and dihedral angles of $\mathbf{4}^+$ are very similar to those of $\mathbf{2}^+$, suggesting that the effects caused by the changes in the ligand from dppe to dfppe are negligible in the view point of geometries around copper centre. The P-Cu-P angles of $\mathbf{2}^+$, $\mathbf{4}^+$, $\mathbf{5}^+$, $\mathbf{6}^+$, and $\mathbf{7}^+$ are in a range from 90° to 92°, which are smaller than those of $[Cu(dmp)(dppp)]^+$ (105.42(3)° and 105.31(3)°) and $[Cu(dmp)(DPEPhos)]^+$ (116.44(4)°). The dihedral angles between N-Cu-N and P-Cu-P planes, α, of $\mathbf{2}^+$, $\mathbf{4}^+$, $\mathbf{5}^+$, and $\mathbf{6}^+$ (85–88°) are similar to those of $[Cu(dmp)(dppe)]^+$ (89.5°, 87.2°) and $[Cu(dmp)(dppp)]^+$ (86.2°, 83.8°), which are characteristic of four-coordinated copper(I) complexes with pseudo-tetrahedral geometry. The dihedral angles of $\mathbf{7}^+$ (82°, 78°) are smaller than the complexes mentioned above, suggesting that the substitution and packing effects can cause distortion from tetrahedral geometry. The dihedral angles of two pyridine planes of bpy moiety, β, of $\mathbf{2}^+$, $\mathbf{4}^+$, $\mathbf{5}^+$, $\mathbf{6}^+$ and $\mathbf{7}^+$ are in a range from 2° to 20°. The volumes of total potential solvent area of $2{\cdot}PF_6$, $4{\cdot}PF_6{\cdot}(CH_3)_2CO$, $5{\cdot}PF_6$, and $7{\cdot}PF_6{\cdot}0.5C_6H_{14}$ per unit cell are 2.5% (91 Å^3/3639 Å^3),

Table 3. Photophysical properties of copper(I) complexes in the solid state at room temperature. The samples were excited at λ_{exc} = 360 nm.

Parameters	**1**·PF_6	**2**·PF_6	**3**·PF_6	**4**·PF_6	**5**·PF_6	**6**·PF_6	**7**·PF_6
λ_{em}/nm	601	583	578	540	519	534	569
τ_{air} [a,b]/μs	0.27(42%) 0.51(58%)	0.18(100%)	0.28(21%) 0.92(79%)	1.0(3%) 5.2(97%)	1.5(9%) 8.0(91%) [d]	0.45(5%) 2.1(95%)	1.3(10%) 5.8(90%)
Φ_{air} [b]/%	<0.5	<0.5	0.6	7	<0.5	3	2
τ_{Ar} [a,c]/μs	0.28(44%), 0.53(56%)	0.19(100%)	0.27(14%) 0.91(86%)	1.1(3%) 6.2(97%)	16(5%) 180(95%) [e]	0.70(9%) 2.7(91%)	1.4(9%) 6.7(91%)
Φ_{Ar} [c]/%	<0.5	<0.5	0.8	8	9	3	2

[a] The decay curves of the emission of the complexes can be fit with a double exponential curve ($I = A_1\exp(-t/\tau_1) + A_2\exp(-t/\tau_2)$) with τ_1 and τ_2, respectively. Parentheses indicate $A_1\tau_1 / (A_1\tau_1 + A_2\tau_2)$ and $A_2\tau_2 / (A_1\tau_1 + A_2\tau_2)$, respectively. [b] Under air. [c] Under argon atmosphere. [d] The emission lifetime of **5**·PF_6 under the oxygen atmosphere is τ_{O2} = 0.27(10%), 2.2(90%) μs. [e] The emission lifetime of **5**·PF_6 under vacuum is τ_{vac} = 18(9%), 169(91%) μs.

8.0% (755 Å^3/9455 Å^3), 9.5% (201 Å^3/2126 Å^3), and 2.7% (241 Å^3/8892 Å^3), respectively. It should be noted that columnar void spaces are obviously present in the crystal of **5**·PF_6 along with both *a* and *c* axes (Figs. 3 and S3). Mann et al. have reported that the quality of the voids is important for the oxygen diffusion which leads to oxygen sensing ability of the emission of the copper(I) complexes; in their case, the voids are lined with and separated by highly mobile CF_3 groups of counterion.[12] These are consistent with the results described in this study, and the presence of the two dimensional columns surrounded by the fluorine atoms can be one of the reasons for the oxygen sensing ability of the photoluminescence of the dfppe complexes. Since the center of the void is present at the special position in the unit cell, the closest hypothetical distance between the oxygen molecule and Cu the center, estimated from the half of the intermolecular distance between two copper atoms, is less than 7.4 Å (Fig. S6). The distance is sufficient for the luminescence quenching by energy transfer from the copper complex to molecular oxygen, because energy transfer of 7.4 Å is much more efficient than that of 30-40 Å where dipole-dipole energy transfer is still comparable with decay of excited state and is related by a factor of sixth power of the distance.[50] Consequently, the location, the size, and the surrounding atoms of the void can affect the oxygen quenching efficiency, because these can affect both the rate of the oxygen diffusion and the rate of energy transfer.

Absorption spectra of all complexes in CH_2Cl_2 show intense absorption around 280 nm due to the π-π* transitions (Fig. 4). Low-energy absorption is clearly observed in the dppe complexes, **1**·PF_6 and **2**·PF_6 (λ_{abs} = 411 nm and 400 nm). The absorption is characteristic of the CT transition (copper and phosphorus → diimine) in a family of copper(I) complexes bearing diimine and diphosphine.[14-19] On the other hands, the corresponding absorption of the dfppe complexes, **3**·PF_6, **4**·PF_6, **5**·PF_6, **6**·PF_6, and **7**·PF_6 is drastically blue-shifted and combined with the π-π* transition.[51] The wavelength at the emission maximum, λ_{em}, of **5**·PF_6 in CH_2Cl_2 solution at room temperature is 550 nm, and the quantum yield of the emission is approximately 0.8% (Figs. S7 and S8). On the other hand, the quantum yields of the luminescence of **1**·PF_6, **2**·PF_6, **3**·PF_6, **4**·PF_6, **6**·PF_6, and **7**·PF_6 were less than 0.1%. The wavelength, quantum yield, and lifetime of the emission of **5**·PF_6 are characteristic of the luminescence based on CT of copper(I) complexes bearing diimine and diphosphine.[14-18] The enhancement of the luminescence of **5**·PF_6 compared to other complexes is typical for the copper(I) complexes bearing diimine, because the methyl substitutions toward the metal centre are known to inhibit both the structural rearrangement and the solvent coordination quenching in the photoexcited states.[14-18]

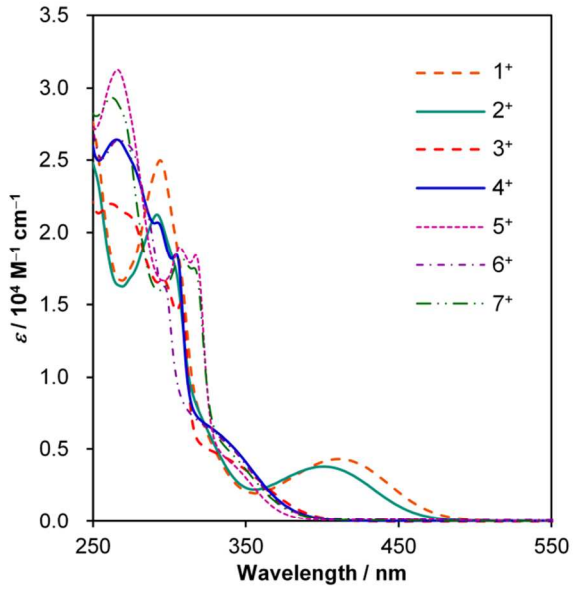

Fig. 4. The absorption spectra of the complexes in air-saturated CH_2Cl_2 at room temperature.

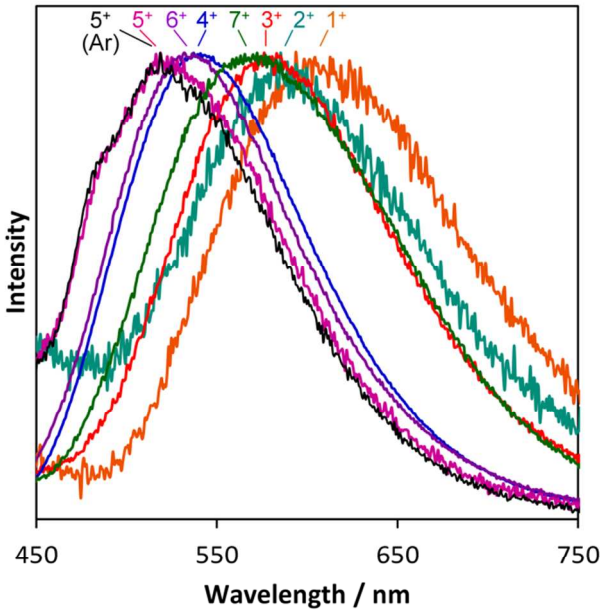

Fig. 5. The emission spectra of the complexes in the solid state at room temperature under air (without notes, λ_{exc} = 370 nm) and under argon atmosphere (**5**$^+$ (Ar), λ_{exc} = 360 nm).

Luminescence spectra of the complexes in the solid state under air at room temperature are shown in Fig. 5, and the photophysical data of the complexes such as the wavelength at the emission maximum (λ_{em}), the lifetime (τ), and the quantum yields (Φ) of the photoluminescence are tabulated in Table 3. All complexes exhibit broad emission band due to the CT excited state, which is characteristic of a family of $[Cu(diimine)(diphosphine)]^+$ complexes. The decay curves of the emission of the present complexes in the solid state can be fit with a double exponential function except that of **2**·PF_6 which can be fit with a single exponential function (Table 3). The double exponential decay curve in the solid state due to aggregation has been reported.[28] The emission of all complexes decays microseconds, which is characteristic of the luminescence of the copper(I) complexes bearing diimine at room temperature

The luminescence of the dfppe complexes has higher energy, longer lifetime, and larger quantum yields than those of dppe complexes (Table 3); this should be rationalized by following factors: (i) Lowering the energy level of HOMO and other occupied orbitals related to the transitions caused by the introduction of the electron-withdrawing pentafluorophenyl groups, (ii) The inhibition of the structural rearrangement in the excited state caused by the enhancement of the bulkiness in the diphosphine moiety from proton to fluorine atoms. These factors should result in the blue-shift of the luminescence, which leads to both longer lifetime and larger quantum yields due to the energy gap law.

The introduction of the electron-donating methyl group substitutions which increase the energy level of LUMO and other orbitals related to diimine moiety. For example, λ_{em} of **1**·PF_6 and **2**·PF_6 are 601 nm and 583 nm, respectively (Table 3). The blue-shift caused by the methyl substitution is also observed in the dfppe complexes (λ_{em} = 578 nm for **3**·PF_6 and λ_{em} = 540 nm for **4**·PF_6). The values of both τ and Φ of the luminescence of **4**·PF_6, **6**·PF_6, and **7**·PF_6 are much higher than that of **3**·PF_6. One of the reasons for the enhancement caused by the substitutions is packing effects; the inhibition of the structural rearrangement, which induces higher energy, longer lifetimes, and larger quantum yields of the emission, is caused by the substituents. Another possible reason for the enhancement of both τ and Φ is the difference in nature of transitions, discussed in DFT calculation paragraphs. In contrast, τ of **2**·PF_6 is shorter than that of **1**·PF_6, but the difference in the values is small which is consistent with previously reported substitution effects on the photophysics of copper(I) complexes bearing diimine.[14-19]

The luminescence of **5**·PF_6 in the solid state under air has short lifetime and low quantum yield, however, that under argon has a very long lifetime and a large quantum yield (Fig. 6). The emission intensity immediately increases by exposing the glass tube containing the powder of **5**·PF_6 to vacuum, and it decreases to air (Fig. 6a). The time course of the changes in the emission of **5**·PF_6 in the solid state at room temperature by the operation of exposing the sample to vacuum and to air shows good repeatability for the oxygen response (Fig. 6a). The changes in the emission by exposing the powder to air are finished within 0.1 seconds, indicating that the response is very fast (Fig. 6b). The luminescence spectrum of **5**·PF_6 under argon is very similar to that under air (Fig. 5), suggesting that the quenching of the excited state by oxygen molecules play a key role for the oxygen responsive abilities without any chemical degradation. The negligible degradation is supported by the fact

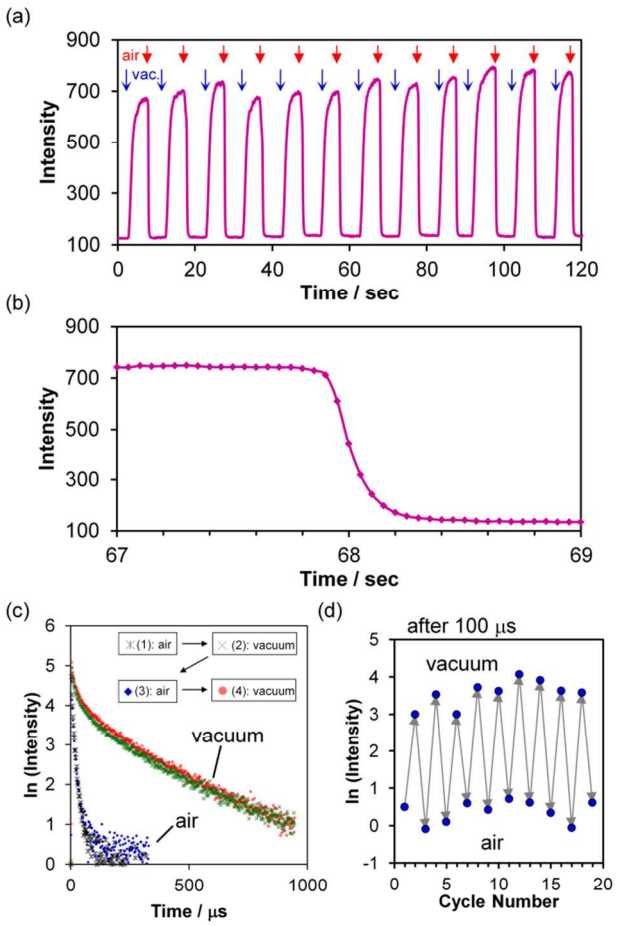

Fig. 6. Oxygen-responsive photoluminescence of **5**·PF_6 in the solid state at room temperature. (a) Time course of the emission intensities upon repeated operations of exposing the sample to vacuum (blue arrows) and to air (red arrows). (b) Magnified graph of (a). Data points are indicated as rhombus. (c) Changes in the luminescence decay curves of **5**·PF_6 upon repeated operations of exposing the sample to vacuum and to air. (d) Changes in the intensity of **5**·PF_6 100 μs after the irradiation of the laser pulse upon repeated operations of exposing the sample to vacuum and to air.

that the IR spectrum of **5**·PF_6 after the repeated operations is almost the same as that before the operations (Fig. S9). The quantum yield of the emission under argon is more than ten times of that under air, indicating that **5**·PF_6 has high sensitivity of the oxygen responsive abilities. The long lifetime in vacuum was recovered after 10 cycles of repeated operations (Figs. 6c and 6d). The lifetimes of τ_1 and τ_2 under vacuum are 18 and 170 μs, which are approximately ten times as large as those under air, suggesting that the oxygen molecules effectively quench the excited state to reduce the lifetime even in the solid state (Table 4). The values under the oxygen are 0.41 and 2.2 μs, which are smaller than that under air, supporting that the oxygen quenching mechanism is operating during the repeatable changes in the luminescence. The values under argon (16 and 180 μs) are almost the same as those under vacuum, supporting that the effects of the other factors such as pressure are very small. The difference in both τ and Φ of **5**·PF_6 between under air and argon is much larger than those of other complexes in the present work, suggesting that the emission of **5**·PF_6 has exceptionally high oxygen responsive abilities.

Table 4. Population analysis of the DFT calculations based on the singlet optimized structures.

	K-S orbital	Energy / eV	Cu[a)]	PP[b)]	NN[c)]
$\mathbf{1}^+$	LUMO+1	-3.77	0	3	97
	LUMO	-4.61	2	2	96
	HOMO	-7.74	51	44	5
	HOMO-1	-8.46	72	8	20
	HOMO-2	-8.72	59	37	4
$\mathbf{2}^+$	LUMO+1	-3.53	0	3	97
	LUMO	-4.44	2	2	96
	HOMO	-7.62	51	43	6
	HOMO-1	-8.32	72	8	20
	HOMO-2	-8.61	63	31	6
$\mathbf{3}^+$	LUMO+1	-4.75	8	92	0
	LUMO	-5.16	2	2	96
	HOMO	-9.18	59	36	5
	HOMO-1	-9.53	67	9	24
	HOMO-2	-10.02	3	2	95
$\mathbf{4}^+$	LUMO+1	-4.66	7	93	0
	LUMO	-4.97	1	2	97
	HOMO	-9.05	58	35	7
	HOMO-1	-9.39	67	9	24
	HOMO-2	-9.83	3	1	96
$\mathbf{5}^+$	LUMO+1	-4.72	2	97	1
	LUMO	-4.98	0	3	97
	HOMO	-9.13	62	33	5
	HOMO-1	-9.43	66	8	26
	HOMO-2	-9.68	1	0	99
$\mathbf{6}^+$	LUMO+1	-4.63	6	91	3
	LUMO	-4.72	1	5	94
	HOMO	-8.93	54	34	12
	HOMO-1	-9.32	67	9	24
	HOMO-2	-9.79	19	1	80
$\mathbf{7}^+$	LUMO+1	-4.69	7	93	0
	LUMO	-4.96	2	2	96
	HOMO	-9.09	59	35	6
	HOMO-1	-9.42	65	10	25
	HOMO-2	-9.59	2	1	97

[a] Components for copper moieties / %. [b] Components for diphosphine moieties / %. [c] Components for diimine moieties / %.

The oxygen responsive luminescence would be observed when the compounds are satisfied two factors, very long lifetime and oxygen-accessible voids. The former factor is satisfied only in $\mathbf{5}\cdot PF_6$ in the present work, because the methyl groups toward the metal centre drastically increase the lifetime of the emission through the inhibition of the structural rearrangement in the excited state. The latter factor is satisfied in case of $\mathbf{5}\cdot PF_6$, because the solid has oxygen-accessible voids. These are consistent with previously reported mechanisms of oxygen responsive emission in the solid state.[10-13] Consequently, the oxygen responsive photoluminescence is obviously observed only by using the powder of $\mathbf{5}\cdot PF_6$.

The value of the lifetime of the luminescence of $\mathbf{5}\cdot PF_6$ under argon in the solid state is in the order of a hundred microseconds, and much larger than those of other complexes (Table 3) under both air and argon atmospheres. The lifetime of $\mathbf{5}\cdot PF_6$ is one of the longest values in a family of copper(I) complexes bearing diimine and diphosphine. One of the reasons for the exceptionally long-lived luminescence is the efficient inhibition of the structural rearrangement in the excited state caused by the methyl substitution toward metal centre, which is well-known for typical copper(I) complexes.[14-19]

The results of DFT calculations for the complexes are tabulated in Table 4 and Table 5, and the Kohn-Sham orbitals are displayed in Fig. 7. Details of the results of the calculations are shown in Figs. S10, S11, and Tables S1 and S2. The optimized structures in the singlet ground state (S_0) of the complexes were used for the population analysis and TDDFT calculations.

HOMO and HOMO-1 of the dfppe complexes ($\mathbf{3}^+$, $\mathbf{4}^+$, $\mathbf{5}^+$, $\mathbf{6}^+$ and $\mathbf{7}^+$) are mainly based on the copper and the phosphorus atomic orbitals. The diimine ligand mainly contributes to HOMO-2 and LUMO, and the diphosphine ligand contributes to LUMO+1 and LUMO+2, since the electron-withdrawing pentafluorophenyl groups decrease the energy level of diphosphine. Despite the components of HOMO, HOMO-1, HOMO-2, and LUMO of dfppe complexes are similar to those of dppe complexes ($\mathbf{1}^+$ and $\mathbf{2}^+$), LUMO+1 and LUMO+2 are different from those of dppe complexes which consist of the atomic orbitals in the diimine moieties.

TDDFT calculation for all complexes in the present work (Table 5) indicates that the largest component of the transition from ground (S_0) to the singlet lowest-lying excited (S_1) state ($S_0 \rightarrow S_1$) is HOMO→LUMO, which can be represented as a CT transition from an orbital consist of copper and phosphorous atomic orbitals to π* orbitals of diimine moiety ($CT_{Cu+P\rightarrow NN}$). The calculated energies of $S_0 \rightarrow S_1$ of dfppe complexes ($\mathbf{3}^+$, 376 nm; $\mathbf{4}^+$, 370 nm; $\mathbf{5}^+$, 360 nm; $\mathbf{6}^+$, 355 nm; $\mathbf{7}^+$, 366 nm) are largely blue-shifted from those of dppe complexes ($\mathbf{1}^+$, 485 nm; $\mathbf{2}^+$, 477 nm), therefore, the blue-shift of the experimental values of the absorption maximum by using dfppe ligand attribute to the difference in the energy of the $CT_{Cu+P\rightarrow NN}$ transitions. The introduction of the electron-withdrawing pentafluorophenyl groups decreases the energy level of electron-occupied orbitals related to diphosphine moiety such as HOMO, therefore, the energy gap between ground and excited states, which reflects the energy of the luminescence, of dfppe complexes are larger than that of dppe complexes. Both $CT_{Cu+P\rightarrow NN}$ and a CT transition from an orbital consist of copper and phosphorous atomic orbitals to diphosphine moieties ($CT_{Cu+P\rightarrow PP}$), such as HOMO→LUMO+1, contribute to the transition from ground to singlet second lowest-lying excited ($S_0 \rightarrow S_2$) of the dfppe complexes. The calculated energies of $S_0 \rightarrow S_2$ are close to those of $S_0 \rightarrow S_1$, $CT_{Cu+P\rightarrow PP}$ can considerably affect the photophysics of dfppe complexes.

Although the largest contributions to the lowest triplet excited states ($S_0 \rightarrow T_1$) of dppe complexes are $CT_{Cu+P\rightarrow NN}$, those of dfppe complexes are the π-π* state in diimine moiety, such as HOMO–2→LUMO. The large contribution of ^{3}π-π* can be one of the reasons for very long lifetime of $\mathbf{5}\cdot PF_6$; the effects have been reported in some copper(I) complexes bearing diimine ligands.[13,29b] The calculated energies of $S_0 \rightarrow T_1$ of dfppe complexes, $\mathbf{3}^+$, $\mathbf{4}^+$, $\mathbf{5}^+$, $\mathbf{6}^+$, and $\mathbf{7}^+$ are 401, 401, 417, 391, and 418 nm, respectively, which are largely blue-shifted from those of dppe complexes ($\mathbf{1}^+$, 541 nm; $\mathbf{2}^+$, 527 nm). These results are consistent with the fact that electronic factors are one of the reasons why the emission spectra of the dfppe complexes are blue-shifted from those of the dppe complexes. The small differences in the calculated energies between $S_0 \rightarrow T_2$ and $S_0 \rightarrow T_1$ are characteristic of dfppe complexes. Since structured emission spectrum is typically observed in case of π-π* transition,[23b, 23c] the π-π* state should not dominate the actual triplet excited state. The fact that the emission of the dfppe complexes ($\mathbf{3}^+$ - $\mathbf{7}^+$) have longer lifetime than those of the dppe complexes ($\mathbf{1}^+$, $\mathbf{2}^+$) may indicate that there is some contributions of the π-π* character in addition to the $CT_{Cu+P\rightarrow NN}$, and $CT_{Cu+P\rightarrow PP}$ nature of the triplet excited state.

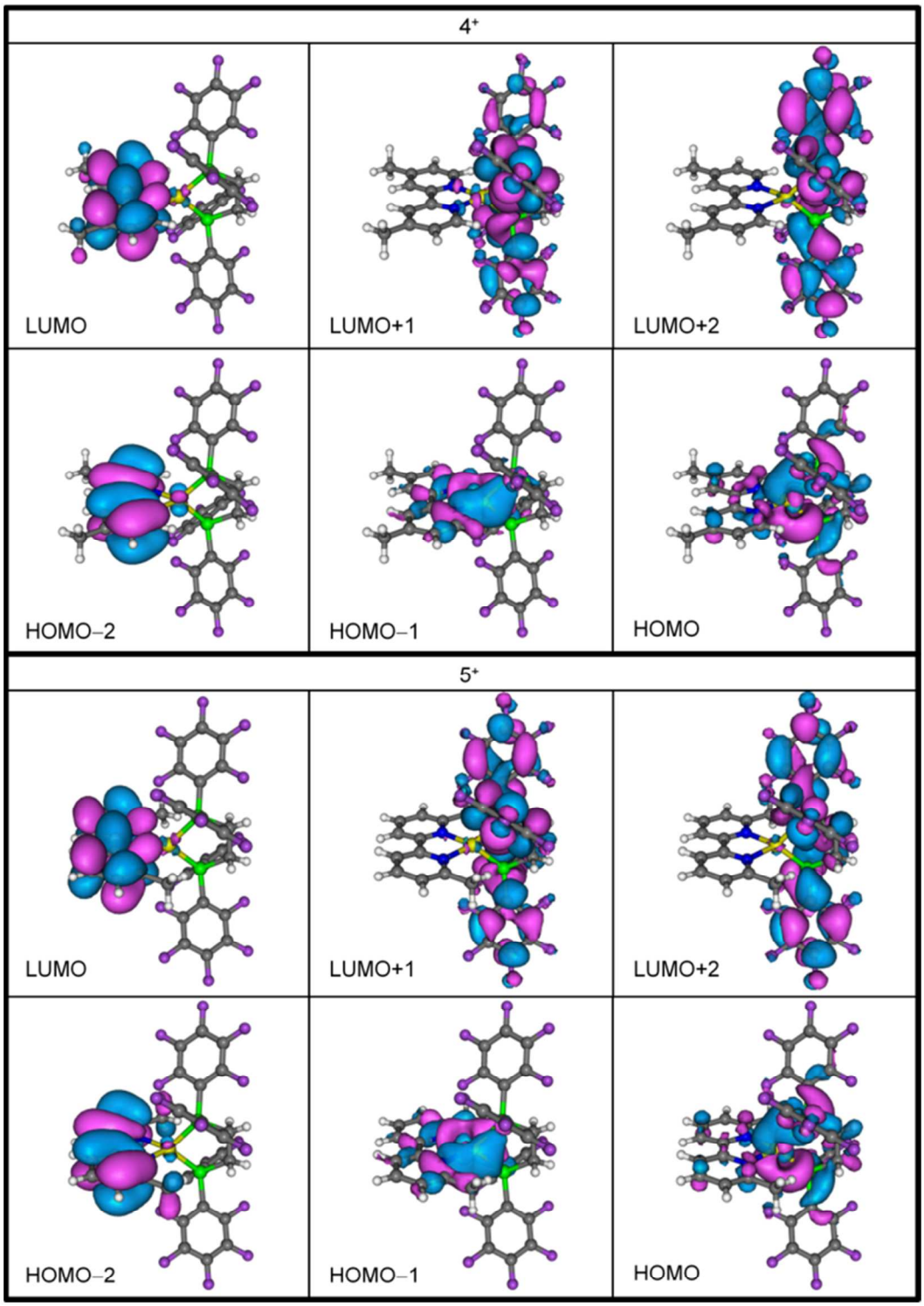

Fig. 7. Kohn-Sham orbitals of $\mathbf{4}^+$ and $\mathbf{5}^+$. Orbitals calculated based on the optimized structure in the S_0 (singlet ground) states (contour value 0.02).

Conclusion

In conclusion, we newly synthesized several copper(I) complexes bearing a fluorinated diphosphine, dfppe, and a bipyridine-type ligand, and characterized by elemental analysis and X-ray structural analysis. The introduction of the methyl substitutions at 4- and 4′- positions dramatically enhances the luminescence of the complexes in the solid state, considering that the luminescence of $\mathbf{4}\cdot PF_6$ is much stronger than that of $\mathbf{3}\cdot PF_6$. The solid of $\mathbf{5}\cdot PF_6$ exhibits very weak luminescence under air, but it exhibits strong luminescence under argon. The lifetime of $\mathbf{5}\cdot PF_6$ in the solid state is also highly oxygen responsive (τ_{air} = 1.5 μs, 8.0 μs, τ_{argon} = 16 μs, 180 μs) due to quenching of the long-lived excited state. The latter lifetime is one of the longest values among all copper(I) complexes

bearing two bidentate ligands, diimine and diphosphine. The introduction of pentafluorophenyl groups induces the decrease in the energy level of the occupied orbitals such as HOMO, and triplet π-π* excited state is important for the photophysics. The responsive abilities attribute to both the very long lifetime of the excited states and the presence of the void space of the crystal. This finding provides not only the significant importance of the luminescence in the solid state under argon for the study of photophysical properties but also the application of highly oxygen responsive sensors with high stability and fast responses.

Acknowledgements

This work was financially supported by Grants-in-Aid from MEXT of Japan (26410077) and the Grant from the Faculty of Science and Technology, Seikei University

Notes and references

Department of Materials and Life Science, Seikei University, Kichijoji-kitamachi, Musashino, Tokyo 180-8633, Japan. E-mail: tsubomura@st.seikei.ac.jp; Fax: +81-422-37-3871; Tel. +81-422-37-3752.
Electronic Supplementary Information (ESI) available: Crystallographic data for X-ray structural analysis, NMR spectra, emission spectra, and details of the DFT calculations. See DOI: 10.1039/b000000x/

1 S. Campagna, F. Puntoriero, F. Nastasi, G. Bergamini and V. Balzani, *Top. Curr. Chem.*, 2007, **280**, 117–214.
2 M. A. Baldo, D. F. O'Brien, Y. You, A. Shoustikov, S. Sibley, M. E. Thompson and S. R. Forrest, *Nature*, 1998, **395**, 151–154.
3 M. A. Baldo, M. E. Thompson and S. R. Forrest, *Nature*, 2000, **403**, 750–753.
4 J.-P. Collin, C. Dietrich-Buchecker, P. Gaviña, M. C. Jiménez-Molero and J.-P. Sauvage, *Acc. Chem. Res.*, 2001, **34**, 477–487.
5 M. Nishikawa, K. Nomoto, S. Kume and H. Nishihara, *J. Am. Chem. Soc.*, 2012, **134**, 10543–10553.
6 T. J. Meyer, *Acc. Chem. Res.*, 1989, **22**, 163–170.
7 J. N. Demas, B. A. DeGraff and P. B. Coleman, *Anal. Chem.* 1999, **71**, 793A.
8 R. Gao, D. G. Ho, B. Hernandez, M. Selke, D. Murphy, P. I. Djurovich and M. E. Thompson, *J. Am. Chem. Soc.*, 2002, **124**, 14828–14829.
9 Leventis, N.; Elder, I. A.; Rolison, D. R.; Anderson, M. L.; Merzbacher, C. I. *Chem. Mater.* **1999**, *11*, 2837.
10 K. A. McGee and K. R. Mann, *J. Am. Chem. Soc.*, 2009, **131**, 1896–1902.
11 C. S. Smith and K. R. Mann, *Chem. Mater.*, 2009, **21**, 5042–5049.
12 C. S. Smith, C. W. Branham, B. J. Marquardt and K. R. Mann, *J. Am. Chem. Soc.*, 2010, **132**, 14079–14085.
13 C. S. Smith and K. R. Mann, *J. Am. Chem. Soc.*, 2012, **134**, 8786–8789.
14 A. Barbieri, G. Accorsi and N. Armaroli *Chem. Commun.*, 2008, 2185–2193.
15 M. Ruthkosky, C. A. Kelly, F. N. Castellano and G. J. Meyer, *Coord. Chem. Rev.*, 1998, **171**, 309–322.
16 N. Armaroli, G. Accorsi, F. Cardinali and A. Listorti, *Top. Curr. Chem.*, 2007, **280**, 69–115.

Table 5. TDDFT results of the complexes. Calculated transition wavelength, oscillator strength (*f*), components of singlet and triplet excited states using the singlet optimized structures are shown. Details of the calculation results are shown in Supporting Information Table S*.

	Singlets calculated using singlet-optimized structures[a]				Triplets calculated using singlet-optimized structures[a]		
	λ / nm	*f*	Components[b]	Coefficients	λ / nm	Components[b]	Coefficients
1$^+$	485	0.0913	HOMO→LUMO	0.68	541	HOMO→LUMO	0.71
	433	0.0016	HOMO-1→LUMO	0.69	458	HOMO-1→LUMO	0.70
2$^+$	477	0.1005	HOMO→LUMO	0.68	527	HOMO→LUMO	0.71
	426	0.0014	HOMO-1→LUMO	0.69	443	HOMO-1→LUMO+1	0.70
3$^+$	376	0.0446	HOMO-1→LUMO	-0.36	401	HOMO-2→LUMO	0.69
			HOMO→LUMO	0.59		HOMO-2→LUMO+5	0.24
	361	0.0369	HOMO-1→LUMO	0.58	398	HOMO-1→LUMO	-0.26
			HOMO→LUMO	0.36		HOMO→LUMO	0.65
4$^+$	370	0.0507	HOMO-1→LUMO	-0.34	401	HOMO-2→LUMO	0.70
			HOMO→LUMO	0.61			
	355	0.0339	HOMO-1→LUMO	0.55	391	HOMO-1→LUMO	-0.21
			HOMO→LUMO	0.31		HOMO→LUMO	0.66
			HOMO→LUMO+1	-0.21			
5$^+$	360	0.0530	HOMO-1→LUMO	-0.27	417	HOMO-2→LUMO	0.71
			HOMO→LUMO	0.63			
	353	0.0124	HOMO-1→LUMO	0.61	380	HOMO→LUMO	0.38
			HOMO→LUMO	0.27		HOMO→LUMO+1	0.33
						HOMO→LUMO+3	0.45
6$^+$	355	0.0091	HOMO→LUMO	-0.38	391	HOMO→LUMO	-0.25
			HOMO→LUMO+1	0.46		HOMO→LUMO+1	0.49
			HOMO→LUMO+3	-0.34		HOMO→LUMO+3	-0.35
	351	0.0515	HOMO-1→LUMO	-0.23	378	HOMO-4→LUMO	0.53
			HOMO→LUMO	0.56		HOMO-3→LUMO	-0.27
			HOMO→LUMO+1	0.30			
7$^+$	366	0.0369	HOMO-1→LUMO	-0.38	418	HOMO-2→LUMO	0.71
			HOMO→LUMO+1	0.58			
	352	0.0258	HOMO-1→LUMO	0.47	388	HOMO-1→LUMO	-0.29
			HOMO→LUMO	0.34		HOMO→LUMO	0.38
			HOMO→LUMO+1	0.28			

[a] First two transitions, $S_0 \rightarrow S_1$, $S_0 \rightarrow S_2$, $S_0 \rightarrow T_1$, and $S_0 \rightarrow T_2$ are shown in this table. [b] Components with coefficients up to 0.2 are shown in this table.

17 A. Lavie-Cambot, M. Cantuel, Y. Leydet, G. Jonusauskas, D. M. Bassani and N. D. McClenaghan, *Coord. Chem. Rev.*, 2008, **252**, 2572–2584.

18 D. R. McMillin and K. M. McNett, *Chem. Rev.*, 1998, **98**, 1201–1219.

19 M. Mohankumar, F. Monti, M. Holler, F. Niess, B. D. Nicot, N. Armaroli, J.-P. Sauvage and J.-F. Nierengarten, *Chem. Eur. J.*, 2014, **20**, 12083-12090.

20 M. Nishikawa, K. Nomoto, S. Kume, K. Inoue, M. Sakai, M. Fujii and H. Nishihara, *J. Am. Chem. Soc.*, 2010, **132**, 9579–9581.

21 Y. Hattori, M. Nishikawa, T. Kusamoto, S. Kume and H. Nishihara *Inorg. Chem.*, 2014, **53**, 2831−2840.

22 (a) D. G. Cuttell, S. M. Kuang, P. E. Fanwick, D. R. McMillin, and R. A. Walton, *J. Am. Chem. Soc.*, 2002, **124**, 6–7. (b) S. M. Kuang, D. G. Cuttell, D. R. McMillin, P. E. Fanwick and R. A. Walton, *Inorg. Chem.*, 2002, **41**, 3313–3322.

23 (a) A. A. Del Paggio and D. R. McMillin, *Inorg. Chem.*, 1983, **22**, 691. (b) C. E. A. Palmer; D. R. McMillin, *Inorg. Chem.*, 1987, **26**, 3837-3840. (c) R. A. Rader, D. R. McMillin, M. T. Buckner, T. G. Matthews, D. J., Jr. Casadonte, R. K. Lengel, S. B. Whittaker, L. M. Darmon, F. E. Lytle *J. Am. Chem. Soc.* 1981, **103**, 5906-5912.

24 R. D. Costa, D. Tordera, E. Ortí, H. J. Bolink, J. Schönle, S. Graber, C. E. Housecroft, E. C. Constable and J. A. Zampese, *J. Mater. Chem.*, 2011, **21**, 16108−16118.

25 Andrés-Tomé, I.; Fyson, J.; Dias, F. B.; Monkman, A. P.; Iacobellis, G.; Coppo, P. *Dalton Trans.* 2012, **41**, 8669−8674.

26 E. C. Constable, C. E. Housecroft, P. Kopecky, E. Schönhofer and J. A. Zampese, *CrystEngComm.*, 2011, **13**, 2742.

27 X.-L. Li, Y.-B. Ai, B. Yang, J. Chen, M. Tan, X.-L. Xin and Y.-H. Shi, *Polyhedron*, 2012, **35**, 47.

28 N. Armaroli, G. Accorsi, M. Holler, O. Moudam, J.-F. Nierengarten, Z. Zhou, R. T. Wegh and R. Welter, *Adv. Mater.*, 2006, **18**, 1313–1316.

29 (a) Z. A. Siddique, Y. Yamamoto, T. Ohno and K. Nozaki, *Inorg. Chem.*, 2003, **42**, 6366-6378. (b) Q. Zhang, T. Komino, S. Huang, S. Matsunami, K. Goushi and C. Adachi, *Adv. Funct. Mater.*, 2012, **22**, 2327–2336. (c) M. S. Asano, K. Tomiduka, K. Sekizawa, K. Yamashita and K. Sugiura, *Chem. Lett.*, 2010, **39**, 376–378.

30 C. T. Cunningham, J. J. Moore, K. L. H. Cunningham, P. E. Fanwick and D. R. McMillin *Inorg. Chem.*, 2000, **39**, 3638.

31 K. Saito, T. Tsukuda and T. Tsubomura, *Bull. Chem. Soc. Jpn.*, 2006, **79**, 437.

32 K. Saito, T. Arai, N. Takahashi, T. Tsukuda and T. Tsubomura, *Dalton Trans.*, 2006, 4444.

33 M. Nishikawa and T. Tsubomura *Bull. Chem. Soc. Jpn.*, 2014, **87**, 912-914.

34 M. Nishikawa, S. Sawamura, A. Haraguchi, J. Morikubo, K. Takao and T. Tsubomura *Dalton Trans.*, **2015**, 44, 411-418..

35 R. M. Bellabarba, M. Nieuwenhuyzen, G. C. Saunders *Organometallics*, 2002, **21**, 5726-5737.

36 T. Korenaga, K. Abe, A. Ko, R. Maenishi and T. Sakai *Organometallics*, 2010, **29**, 4025-4035.

37 (a) G. J. Kubas, *Inorg. Synth.*, 1979, **19**, 90–92.

38 (a) G. R. Fulmer, A. J. M. Miller, N. H. Sherden, H. E. Gottlieb, A. Nudelman, B. M. Stoltz, J. E. Bercaw, and K. I. Goldberg, *Organometallics*, 2010, **29**, 2176–2179. (b) A. Higelin, C. Haber, S. Meier, I. Krossing *Dalton Trans.* **2012**, 41, 12011–12015.

39 K. Suzuki, A. Kobayashi, S. Kaneko, K. Takehira, T. Yoshihara, H. Ishida, Y. Shiina, S. Oishi, and S. Tobita, *Phys. Chem. Chem. Phys.*, 2009, **11**, 9850.

40 (a) Rigaku (2000). *CrystalClear*. Rigaku Corporation, Tokyo, Japan. (b) A. Altomare, G. Cascarano, C. Giacovazzo, A. Guagliardi, M. C. Burla, G. Polidori and M. Camalli, *J. Appl. Crystallogr.*, 1994, **27**, 435–436. (c) G. M. Sheldrick, *Acta Crystallogr., Sect. A: Fundam. Crystallogr.*, 2007, **64**, 112–122. (d) Rigaku Corporation, *CrystalStructure*, Tokyo, Japan. (e) Farrugia, L. J. *J. Appl. Cryst.* 1999, 32, 837–838. (f) P. van der Sluis and A. L. Spek, *Acta Crystallogr., Sect. A: Fundam. Crystallogr.*, **1990**, 46, 194–201.

41 M. J. Frisch, G. W. Trucks, H. B. Schlegel, G. E. Scuseria, M. A. Robb, J. R. Cheeseman, J. A. Montgomery, Jr., T. Vreven, K. N. Kudin, J. C. Burant, J. M. Millam, S. S. Iyengar, J. Tomasi, V. Barone, B. Mennucci, M. Cossi, G. Scalmani, N. Rega, G. A. Petersson, H. Nakatsuji, M. Hada, M. Ehara, K. Toyota, R. Fukuda, J. Hasegawa, M. Ishida, T. Nakajima, Y. Honda, O. Kitao, H. Nakai, M. Klene, X. Li, J. E. Knox, H. P. Hratchian, J. B. Cross, V. Bakken, C. Adamo, J. Jaramillo, R. Gomperts, R. E. Stratmann, O. Yazyev, A. J. Austin, R. Cammi, C. Pomelli, J. W. Ochterski, P. Y. Ayala, K. Morokuma, G. A. Voth, P. Salvador, J. J. Dannenberg, V. G. Zakrzewski, S. Dapprich, A. D. Daniels, M. C. Strain, O. Farkas, D. K. Malick, A. D. Rabuck, K. Raghavachari, J. B. Foresman, J. V. Ortiz, Q. Cui, A. G. Baboul, S. Clifford, J. Cioslowski, B. B. Stefanov, G. Liu, A. Liashenko, P. Piskorz, I. Komaromi, R. L. Martin, D. J. Fox, T. Keith, M. A. Al-Laham, C. Y. Peng, A. Nanayakkara, M. Challacombe, P. M. W. Gill, B. Johnson, W. Chen, M. W. Wong, C. Gonzalez, and J. A. Pople, Gaussian, Inc., Wallingford CT, 2004.

42 A. D. J. Beck, *Chem. Phys.*, 1992, **96**, 2155‑2160.

43 A. D. J. Becke, *Chem. Phys.*, 1993, **98**, 5648‑5652.

44 C. Lee, W. Yang and R. G. Parr, *Phys. Rev.*, 1988, **B37**, 785.

45 A. J. H. Wachters, *J. Chem. Phys.*, 1970, **52**, 1033‑1036.

46 S. I. Gorelsky, *AOMix*: Program for Molecular Orbital Analysis, University of Ottawa, 2011.

47 U. Varetto, *Molekel*, Swiss National Supercomputing Centre: Lugano, Switzerland.

48 We made best efforts to prepare [Cu(6dmbpy)(dppe)]PF_6 by using a procedure similar to that described for **2**·PF_6. [Cu(MeCN)$_4$]PF_6 (112 mg, 0.3 mmol) was added to the dichloromethane solution (5 mL) of dppe (119 mg, 0.3 mmol). Then, 6dmbpy (55 mg, 0.3 mmol) was added. The solution was stirred for 1 h at room temperature, then 7 ml of diethyl ether was slowly added to the solution. The mixture was kept in a refrigerator for an overnight. Red precipitates were obtained by filtration (30 mg). The solids were confirmed by experimental ^{1}H NMR in CD_3CN (Fig. S12) which is same as that for [Cu(6dmbpy)$_2$]PF_6.[49]

49 B. Bozic-Weber, V. Chaurin, E. C. Constable, C. E. Housecroft, M. Meuwly, M. Neuburger, J. A. Rudd, E. Schönhofer and L. Siegfried, *Dalton Trans.*, 2012, **41**, 14157.

50 N. J. Turro, V. Ramamurthy, J. C. Scaiano, *Modern Molecular Photochemistry of Organic Molecules*, University Science Books, Sausalito, California, 2010.

51 The Stokes shifts found for $\mathbf{3}^+$–$\mathbf{7}^+$ were estimated from the wavelength where molar coefficients, ε, are approximately equal to 4×10^3 M cm^{-1}. The stokes shift observed from **5**·PF_6 in solution is 11300 cm^{-1}, which is significantly larger than those of typical copper(I) complexes bearing diimine and diphosphine such as [Cu(dmp)(DPEphos)]$^+$ (8600 cm^{-1}).[22] Moreover, the stokes shifts of the dfppe complexes, **3**·PF_6, **4**·PF_6, **5**·PF_6, **6**·PF_6, and **7**·PF_6 using λ_{abs} in the solution state and λ_{em} in the solid state are 11900 cm^{-1}, 10100 cm^{-1}, 10100 cm^{-1}, 9900 cm^{-1}, and 11300 cm^{-1}, which are much larger than those of the dppe complexes, **1**·PF_6 (7600 cm^{-1}) and **2**·PF_6 (7700 cm^{-1}). These results suggest that the structural reorganizations in the excited state of dfppe complexes are obviously larger than those of dppe complexes.

Long-lived and Oxygen-Responsive Photoluminescence in the Solid State of Copper(I) Complexes Bearing Fluorinated Diphosphine and Bipyridine Ligands

Michihiro Nishikawa, Yuri Wakita, Tatsuya Nishi, Takumi Miura, Taro Tsubomura*

TOC graphic

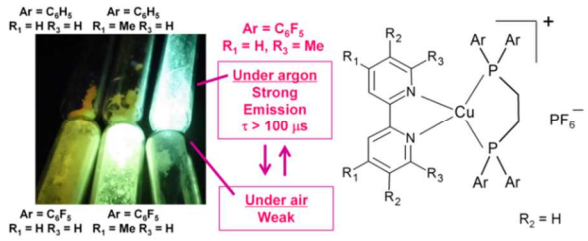

Luminescence properties of a family of newly synthesized copper(I) complexes bearing 2,2′-bipyridine derivative and 1,2-bis(dipentafluorophenyl)phosphinoethane were investigated. The luminescence of a dfppe complex in the solid state is highly oxygen responsive.